Electronic Supplementary Information (ESI) for:

Photoinduced proton transfer inside an engineered green fluorescent protein: A stepwise-concerted-hybrid reaction

Longteng Tang,[1] Yanli Wang,[1] Liangdong Zhu,[1] Karen Kallio,[2] S. James Remington,[2] and Chong Fang[1,*]

[1]Department of Chemistry, Oregon State University, Corvallis, Oregon 97331, USA

[2]Institute of Molecular Biology and Department of Physics, University of Oregon, Eugene, Oregon 97403, USA

* To whom correspondence should be addressed. E-mail: Chong.Fang@oregonstate.edu

This PDF file includes:

ESI figures (S1-S2) followed by additional discussions, and ESI references.

ESI Figures

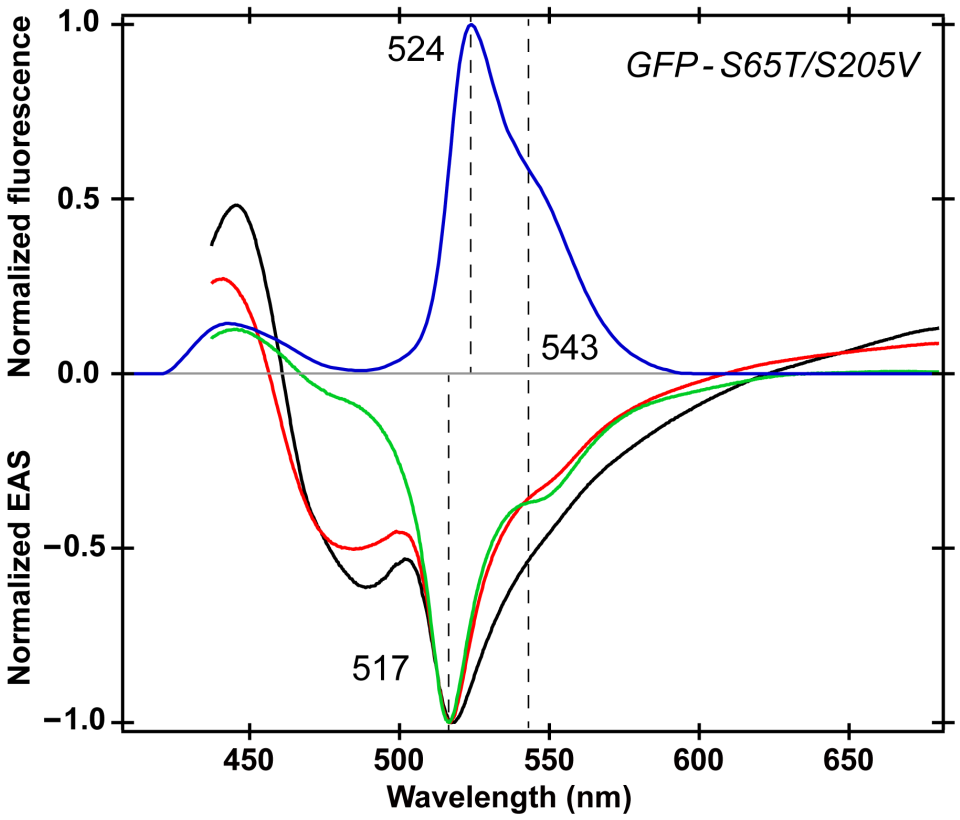

Fig. S1 Normalized fluorescence and evolution-associated spectrum (EAS) of the GFP-S65T/S205V mutant. The comparison between the steady-state emission peaks (blue) and the transient electronic spectra (black, red to green) from global analysis of the fs-TA data corroborates the I* nature of the green EAS. Key band positions are denoted by dashed lines.

The first (black) and second (red) EAS traces exhibit a notable stimulated emission (SE) band near 480 nm that diminishes on the ~100 ps timescale (see main text) after 400 nm photoexcitation, which indicate that the protein chromophore in these two temporal stages has not reached the I* state which relaxes mainly by fluorescence with a ns lifetime.[1,2] The peak position difference between this SE band and the steady-state A* fluorescence peak at ~443 nm arises from the spectral overlap with a nearby excited state absorption (ESA) band below 450 nm, which was

also observed for a widely used GFP mutant with identical photophysical properties as wtGFP but better solubility in water with a diminished deprotonated population.[3] Subsequently, the third (green) trace displays a dominant SE band at ~517 nm while the shoulder fitted at 543 nm becomes apparent, which resembles the fluorescence band profile (blue). The longer wavelength shoulder in the fluorescence spectrum indicates vibronic coupling between spontaneous emission and a 670 cm^{-1} mode that is attributed to a deprotonated chromophore in S_0 (see main text). In contrast, the I* SE band is coupled to a 926 cm^{-1} mode as estimated from the energy gap between 517 and 543 nm. We suspect that after the ESPT barrier crossing from A*→I*, different vibrational modes could be strongly coupled to the downward electronic transition depending upon the relative position of the initial and final states in the PES of I* and I. Since the 543 nm shoulder becomes prominent at later time points as the main 517 nm peak increases its intensity (see Fig. 3), a more relaxed vibrational state in I* is likely involved in the SE transition, and the observed vibronic progression could be attributed to a vibrational mode at ~926 cm^{-1} in S_0, which is close in frequency to a ground state mode at ~916 cm^{-1} mode (see Fig. 5). This S_0 mode consists of in-plane imidazolinone ring deformation and some bridge-H our-of-plane wagging motions from our DFT calculations of a geometrically optimized structure of the deprotonated chromophore.[4] The vibronic involvement of a different vibrational mode in spontaneous emission (Fig. 2) versus stimulated emission (Fig. 3) is a notable experimental result, which suggests that more collective motions of the chromophore two-ring system are active in the transient domain while more imidazolinone ring motions are present in a more relaxed state.[5]

Notably, we used the Glotaran software to perform global analysis of the fs-TA data of this GFP-S65T/S205V mutant after 400 nm photoexcitation.[6,7] The singular value decomposition (SVD) shows two to three major components. Our global analysis with two, three, and four

components yields residual standard error (RSE, equivalent to the root mean square error) of 7.05×10^{-4}, 6.17×10^{-4}, and 6.11×10^{-4}, respectively. This comparison shows a notable reduction of RSE (by ~13%) going from two to three components but a much less/almost negligible reduction of RSE (by ~1%) when an extra component is further added, indicating that three components are necessary and essentially adequate to fit our fs-TA data traces. Based on our prior understanding of the ESPT mechanism in a GFP molecular system with characteristic electronic dynamics,[3,4,8] we found that the EAS analysis provides a better representation of the evolving electronic features than the individual decay-associated spectrum (DAS). Therefore, a sequential model was chosen to analyze our fs-TA data (Fig. 3a) and retrieve the underlying components (Fig. 3b), while the EAS approach typically well reflects the mixtures of molecular states.[9] Further details about the nature of these temporal components in the electronic domain (e.g., "purity" of pertinent species, relevant structural motions) can be elucidated by the species-associated difference spectra (SADS, target analysis)[7] as well as the complementary FSRS spectral analysis along the photoinduced reaction coordinate of the chromophore (see main text).

Moreover, we observed a ~897 cm^{-1} A* mode in the excited-state FSRS with an 800 nm Raman pump. In contrast, the 879 cm^{-1} A* mode in S_1 with a 550 nm Raman pump (Fig. 6a) could be due to the chromophore subpopulation with some deprotonated character and stronger H-bonding interactions with the surrounding partners,[10,11] hence an enlarged quantum "box" for the delocalized electron over the chromophore two-ring conjugated system. Therefore, an effective experimental way to visualize transient atomic motions prior to fluorescence is tunable FSRS with a suitable Raman pump wavelength (see Fig. 6a *versus* Fig. 4a).

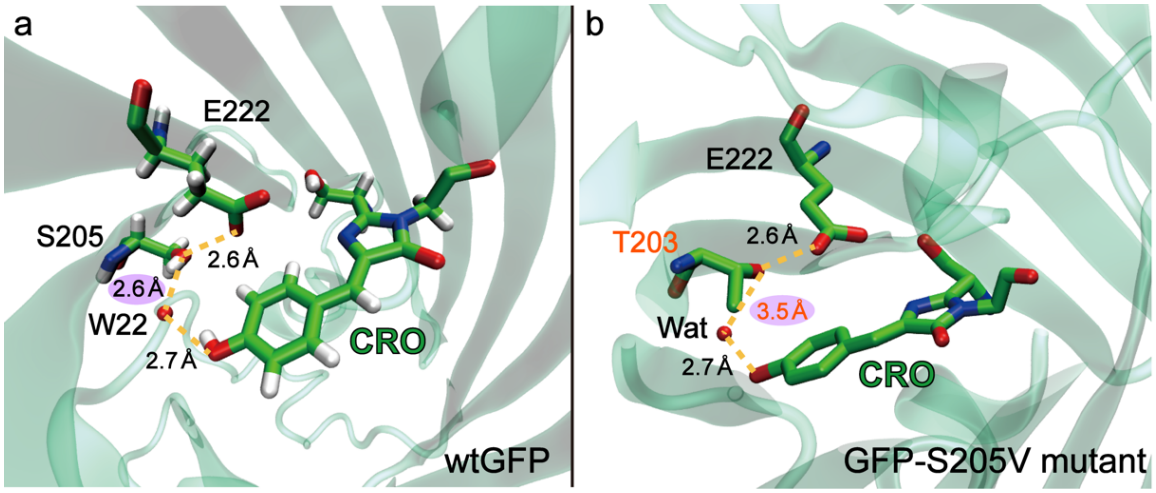

Fig. S2 The proton transfer wire in crystallographic structures of (a) wtGFP (PDB: 2WUR)[12] and (b) the GFP-S205V mutant (PDB: 2QLE).[13] The rearranged T203 residue and the much longer O···O distance between T203 and an adjacent water molecule along the ESPT chain are highlighted in orange. The key differences between the H-bonding distances in angstrom unit are denoted by a semi-transparent magenta ellipse.

Notably, the most significant change of the oxygen-oxygen distance along the ESPT chain is the W22-S205 pair and Wat-T203 pair in wtGFP and the GFP-S205V mutant, respectively. This particular H-bonding chain component does not directly involve the phenolic or imidazolinone end of the embedded chromophore inside the protein pocket, hence could be more susceptible and sensitive to the surrounding protein residue configurations. The close similarity between the other oxygen-oxygen distances along the ESPT chain suggests that the chromophore is more effective in its immediate vicinity to interact with proton donor or acceptor partners, in this case a bridging water molecule on one end and E222 on the other end. Furthermore, the initial small-scale proton motions along with heavy-atom motions on the few ps timescale (see main text) likely occur in the vicinity of the chromophore phenolic end, where an H-bond to the dissociable proton exists at the electronic ground state that could support the ultrafast atomic motions upon photoexcitation.[4,14,15]

ESI References

1 M. Chattoraj, B. A. King, G. U. Bublitz and S. G. Boxer, *Proc. Natl. Acad. Sci. U. S. A.*, 1996, **93**, 8362-8367.

2 K. Brejc, T. K. Sixma, P. A. Kitts, S. R. Kain, R. Y. Tsien, M. Ormö and S. J. Remington, *Proc. Natl. Acad. Sci. U. S. A.*, 1997, **94**, 2306-2311.

3 J. T. M. Kennis, D. S. Larsen, I. H. M. van Stokkum, M. Vengris, J. J. van Thor and R. van Grondelle, *Proc. Natl. Acad. Sci. U. S. A.*, 2004, **101**, 17988-17993.

4 L. Tang, W. Liu, Y. Wang, Y. Zhao, B. G. Oscar, R. E. Campbell and C. Fang, *Chem. Eur. J.*, 2015, **21**, 6481-6490.

5 L. Tang, W. Liu, Y. Wang, L. Zhu, F. Han and C. Fang, *J. Phys. Chem. Lett.*, 2016, **7**, 1225-1230.

6 J. J. Snellenburg, S. Laptenok, R. Seger, K. M. Mullen and I. H. M. van Stokkum, *J. Stat. Softw.*, 2012, **49**, 1-22.

7 C. Chen, W. Liu, M. S. Baranov, N. S. Baleeva, I. V. Yampolsky, L. Zhu, Y. Wang, A. Shamir, K. M. Solntsev and C. Fang, *J. Phys. Chem. Lett.*, 2017, **8**, 5921–5928.

8 C. Fang, R. R. Frontiera, R. Tran and R. A. Mathies, *Nature*, 2009, **462**, 200-204.

9 R. Berera, R. van Grondelle and J. T. M. Kennis, *Photosynth. Res.*, 2009, **101**, 105-118.

10 W. Liu, Y. Wang, L. Tang, B. G. Oscar, L. Zhu and C. Fang, *Chem. Sci.*, 2016, **7**, 5484-5494.

11 R. Simkovitch, S. Shomer, R. Gepshtein and D. Huppert, *J. Phys. Chem. B*, 2015, **119**, 2253-2262.

12 A. Shinobu, G. J. Palm, A. J. Schierbeek and N. Agmon, *J. Am. Chem. Soc.*, 2010, **132**, 11093-11102.

13 X. Shu, P. Leiderman, R. Gepshtein, N. R. Smith, K. Kallio, D. Huppert and S. J. Remington, *Protein Sci.*, 2007, **16**, 2703-2710.

14 M. Rini, B.-Z. Magnes, E. Pines and E. T. J. Nibbering, *Science*, 2003, **301**, 349-352.

15 Y. Wang, L. Tang, W. Liu, Y. Zhao, B. G. Oscar, R. E. Campbell and C. Fang, *J. Phys. Chem. B*, 2015, **119**, 2204-2218.